

## Investigations on non-biodegradable zirconium dioxide reinforced aluminium alloy (AA6081) matrix composite developed by using powder metallurgy route

K. R. Kavitha<sup>a,\*</sup>, S. Prakash<sup>a</sup>, M. Ravichandran<sup>b</sup>

<sup>a</sup>*School of Mechanical Engineering, Sathyabama Institute of Science and Technology, Chennai, India*

<sup>b</sup>*Department of Mechanical Engineering, K. Ramakrishnan College of Engineering, Trichy, 621 112, India*

Aluminium alloy (AA6081) composites reinforced with Zirconium Dioxide ( $ZrO_2$ ) have been produced through Powder Metallurgy (PM). The  $ZrO_2$  particles have been included in the matrix based on the weight percentages to produce various compositions such as AA6081- 2 wt. %  $ZrO_2$ , AA6081- 4 wt. %  $ZrO_2$ , AA6081- 6 wt. %  $ZrO_2$  and AA6081- 8 wt. %  $ZrO_2$ . The Crystallographic Structure of a material and Surface topology and composition analysis was conducted for the green and sintered composite samples. Theoretical density, green and sintered density of the samples has been reported. The wear rate (WR) of the AA6081- 8 wt. %  $ZrO_2$  composite was studied using Pin on disc (POD). Taguchi was applied to study the wear parameters (Load P; Sliding distance D; Sliding velocity V) and the systematic and statistical analysis was conducted by L9 array. The mechanical properties such as hardness, compressive strength (CS) and impact strength was enhanced for the inclusion of  $ZrO_2$  particles in the AA6081 matrix up to 8 wt. %. Wear studies of AA6081- 8 wt. %  $ZrO_2$  composite revealed that the P is the most dominant factor for WR. ANOVA analysis revealed that load is highly contributed parameter for the WR of the PM composite.

(Received May 31, 2021; Accepted July 23, 2021)

*Keywords:* Aluminium, Composite, Properties, Powder metallurgy

### 1. Introduction

Metal matrix composites (MMC) are extensively used materials due its excellent properties and characteristics [1]. Of all MMCs, aluminium alloy matrix composites are highly attractive because of its strength and excellent wear properties compared to the matrix aluminium alloys [2]. AA6081 is one of the 6xxx aluminum series and widely used one because of its mechanical properties and workability [3]. The reinforcing of ceramic or oxide particles improves the mechanical properties of the composites [4]. Recently variety of reinforcement materials are used to produce the MMCs. Zirconium Oxide is one of the effective reinforcement materials to develop AMCs [5]. Ravi Kumar et al developed  $ZrO_2$  and coconut shell ash reinforced AMCs and described that inclusion of reinforcements enhanced the properties [6]. Mostafa Roosta et reported the evaluation of W/ZrC composite and concluded that Conventional  $ZrO_2/WC$  are possess better mechanical properties because of  $ZrO_2$  content [7]. AMMCs are manufactured by the various process such as stir casting [8], squeeze casting, in situ reaction [3], pressure infiltration, powder metallurgy [9] and powder moulding [4]. Though various methods are available, powder metallurgy technique is the most suitable one since it offers uniform distribution of reinforcements and controlled microstructure [10]. Hailong Wang et al analyzed the properties and fracture analysis of the PM SiC/Cu–Al composite and they described that the addition of SiC enhanced the properties of the composites [11]. Meftah Hrairi et al investigated the mechanical and acoustic properties of the composites fabricated by PM-fabricated composites and found that adding fly ash strengthened the properties [12]. Corrochano et al developed  $MoSi_2$  reinforced AMCs and investigated their wear properties, reporting that adding reinforcement improved the composites wear resistance [13]. Cook et al developed Al-TiB<sub>2</sub> composites and investigated their wear properties, concluding that the TiB<sub>2</sub> particles in the matrix decreased the composite's wear [14]. The wear properties of graphite reinforced Al composites were studied by Akhlaghi and Zare-Bidaki. They used in-situ PM approach and found that adding graphite increased wear resistance.

---

\* Corresponding author: kaviraghu07@gmail.com

[15]. The Al-TiC composite formed by Nemati et al, who found that inclusion of TiC improved the hardness and wear properties of the composites [16]. PM was used by Mehdi Rahimian et al to develop Alumina reinforced AMCs and they found that particle size influences the properties and microstructure of the developed hybrid materials [17]. Taguchi method is being extensively used for finding the optimum parameters in numerous areas through simulation [18]. This method is also employed to determine the optimum wear parameters for the composite samples [19]. Beygi et al developed Al<sub>2</sub>O<sub>3</sub> reinforced Fe-Ni composites and they used Taguchi method to optimize the parameters and obtained improved mechanical properties for the composite [20]. Majid Abdellahi et al investigated the parameters to enhance the properties of the ceramic reinforced composite synthesized from ball milling process [21]. Shiva Kumar and Chennakesava Reddy used Taguchi method to study the wear and mechanical behaviors of the Nylon-6/ Boron Nitride polymer composites [22]. Srinivasan et al optimized the PM and extrusion parameters to attain maximum mechanical properties of B4C reinforced AMCs produced via PM route [23].

As a result, the current research aims to manufacture AMCs by reinforcing ZrO<sub>2</sub> material and studying the composites mechanical properties. In addition, the Taguchi technique was used to examine the composite's wear behavior. The sintered and green samples were subjected to microstructure studies using SEM and XRD analysis.

## 2. Experimental Details

Figure 1 displays the complete experimental plan for the present work. Aluminium powders (less than 100 µm) and ZrO<sub>2</sub> particles (less than 100 µm) are purchased for Royal scientific, Trichy India. AA6081 and ZrO<sub>2</sub> particles were mixed in high energy ball mill (Ball diameter 15 mm; Zirconium ball, BPR 3:1; Speed 250 rpm) for the period of 1 h to yield the different compositions. The ball milled composite mixtures were compacted in down-streaming vertical hydraulic press. Then, the green compacts were sintered in atmospheric controlled furnace (570 °C & 2 h). Then the sintered specimens were cleaned and machined for microstructural and mechanical properties studies. XRD and SEM analysis was conducted for the green and sintered samples to study the phase and morphology. The theoretical density of the samples was calculated by using standard formula. Archimedes principle was employed to calculate the green and sintered density of the alloy and composite samples.

Vickers micro hardness tester was employed to perform the hardness test. Emery sheets were used to polish the specimen. The ASTM E384-08 hardness test was performed with a load of 0.3 kg and a dwell time of 10 seconds. Compressive strength was determined for the sintered samples. The compression test was carried out in accordance with ASTM standard E9-89a. The wear test was carried out on the composite with the best mechanical properties. The wear existence of the sample was examined using a pin on disc apparatus. Table 1 shows the result of the experiments. To reduce the wear rate of the AA6081 – 8 wt. percentage ZrO<sub>2</sub> composites, input factors such as load (P) (N), Sliding velocity (V) (m/s), and sliding distance (D) (m) were chosen.



Fig. 1. Experimental plan for the present work.

Table 1. Control parameter and their levels.

Control parameters	Units	Levels		
		1	2	3
P (A)	N	10	20	30
V (B)	m/s	1	2	3
D (C)	m	1000	1500	2000

Table 2. L9 array with output responses and their corresponding S/N ratio.

Experiment Number	P (N)	V (m/s)	D (m)	WR $\times 10^{-3}$ ( $\text{mm}^3/\text{m}$ )	SN Ratio	Mean
1	10	1	1000	6.45	-16.1912	6.45
2	10	2	1500	6.52	-16.2850	6.52
3	10	3	2000	6.64	-16.4434	6.64
4	15	1	1500	6.85	-16.7138	6.85
5	15	2	2000	6.81	-16.6629	6.81
6	15	3	1000	6.92	-16.8021	6.92
7	20	1	2000	6.97	-16.8647	6.97
8	20	2	1000	6.82	-16.6757	6.82
9	20	3	1500	7.02	-16.9267	7.02

### 3. Results and discussion

#### 3.1. SEM analysis of green and sintered samples

The SEM images of the AA6081 and  $\text{ZrO}_2$  reinforced green composites are shown in figure 2 (a-e).

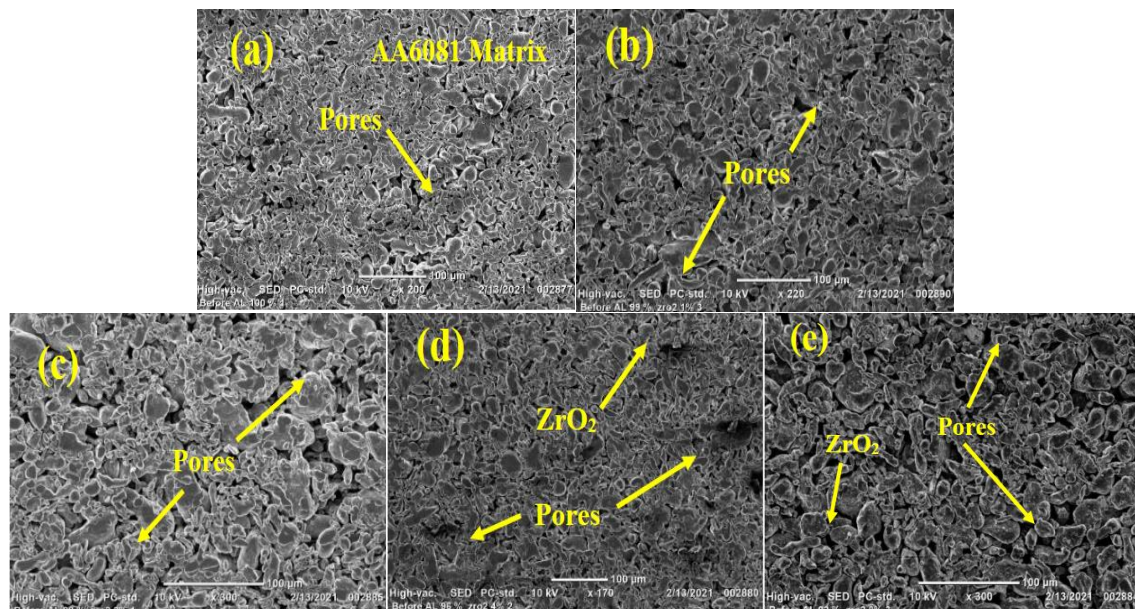


Fig. 2. (a-e) SEM images of the green composite samples.

The SEM image of the AA6081 green compact is shown in Figure 2(a). The picture clearly shows the absence of  $\text{ZrO}_2$  particles. SEM representations of composite samples are shown in Figure 2 (b-e). The introduction of  $\text{ZrO}_2$  particles in amounts of 2% and 4% did not reveal mush

distribution in the matrix. The SEM images of the composite samples containing 6 and 8 wt. percentage are shown in Figure 2 (d) and (e). The presence of  $ZrO_2$  particles is seen and these particles distributed uniformly. When compare with sintered samples, more pores are seen in the green compacts for the alloy and reinforced composites. SEM images of sintered samples are shown in Figure 3 (a-e). Pores are reduced in sintered samples for both alloy and composites samples. The even spreading of  $ZrO_2$  particles in the composites samples can be seen in SEM photographs. The proper spreading of  $ZrO_2$  particles is due to the proper milling parameters, even if the density of the reinforcement is higher than the matrix alloy [24].

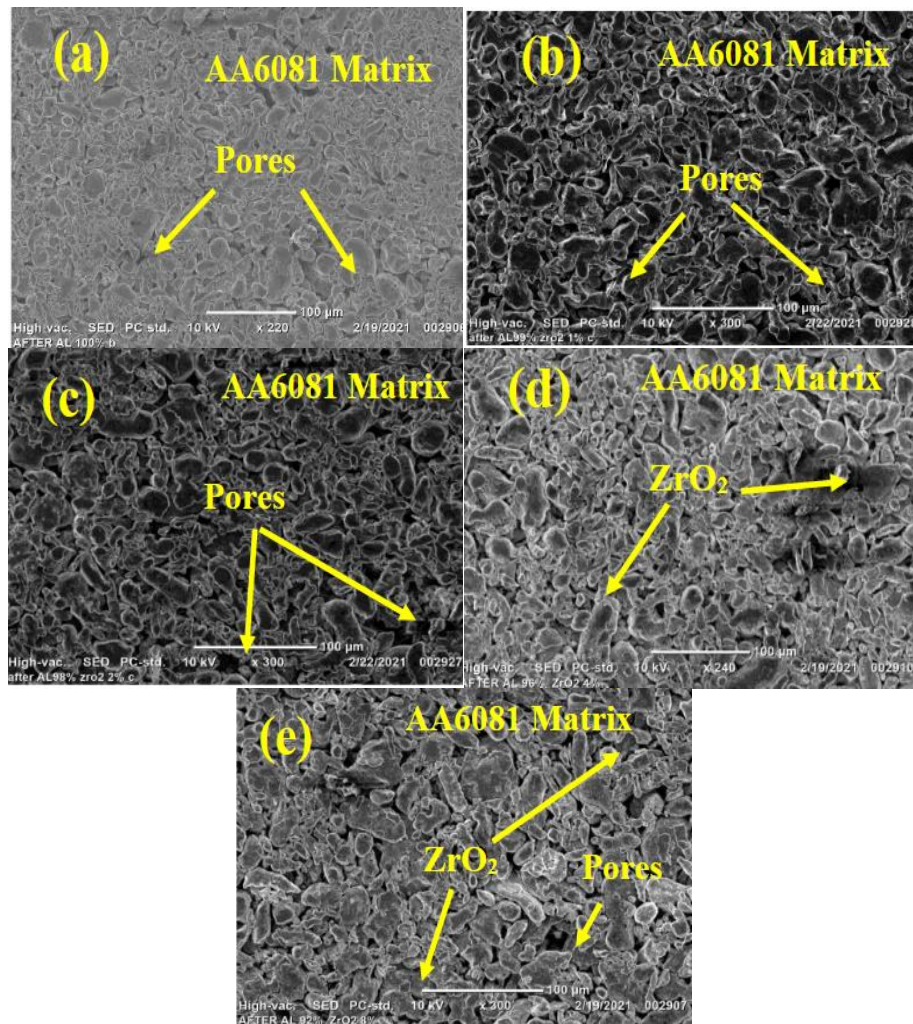


Fig. 3. (a-e) SEM images of the sintered composite samples.

### 3.2. XRD analysis of green and sintered samples

The XRD pattern of the AA6081 and  $ZrO_2$  reinforced green is shown in Figure 4 (a-e). The XRD pattern of the AA6081 green compacts is shown in Figure 4a. The absence of  $ZrO_2$  particles is obvious. The results of composite samples containing 2, 4 and 6 wt. percentage  $ZrO_2$  particles are shown in Figure 4(b-d). Figure 4(b) and 4(c) show that the  $ZrO_2$  peak is missing (c). The existence of  $ZrO_2$  particles in the composite sample with the (111) plane can be seen in Figure 4(d). The XRD pattern of the composite with 8 wt. percentage reinforcement is shown in Figure 4(e) and it clearly shows the  $ZrO_2$  peak with (202) and (113) planes, as well as peak broadening.

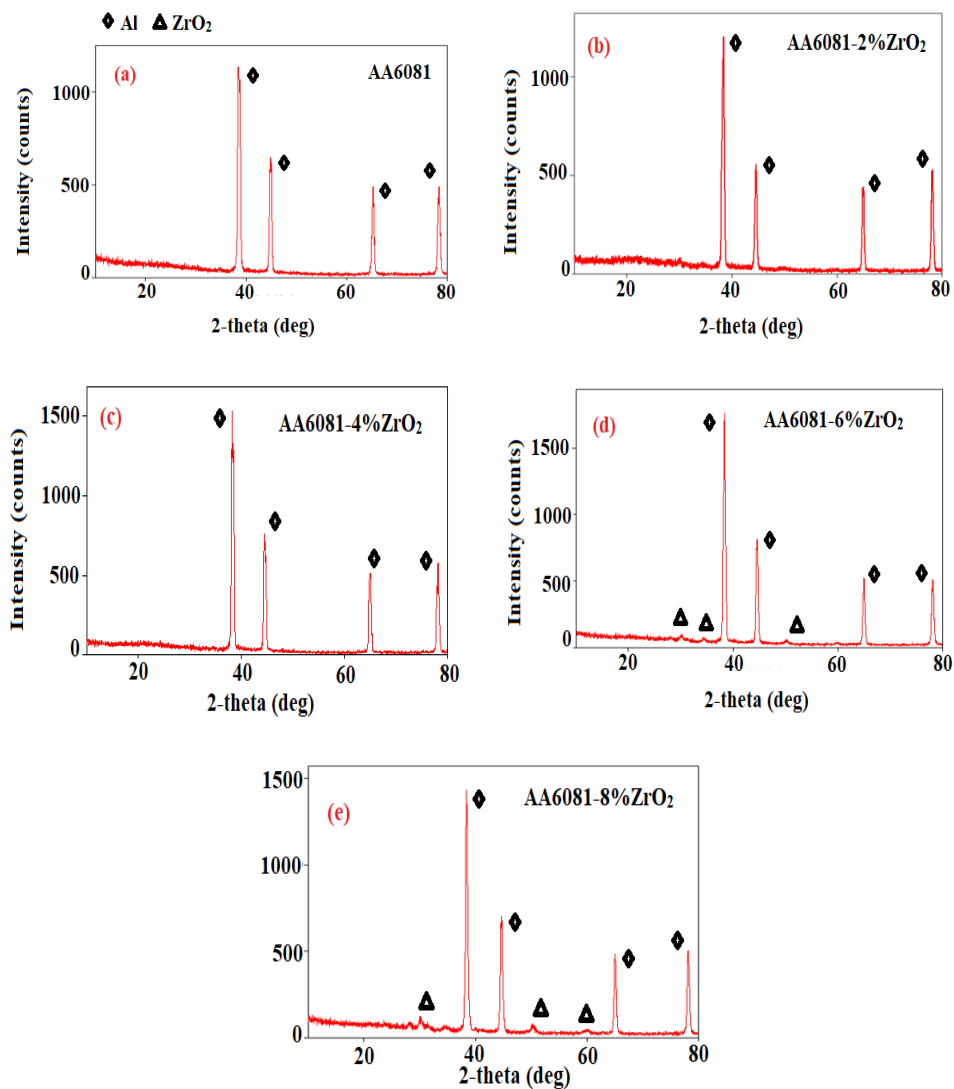


Fig. 4. (a-e) XRD analyses of green AA6081 and composite compacts.

Figure 5 (a-e) displays the XRD pattern of the AA6081 and ZrO<sub>2</sub> reinforced sintered composites. Figure 5(a) displays the XRD analysis of AA6081 alloy sintered samples. The aluminium peak with high intensity is observed and no other elements are observed. The XRD pattern of composite samples shows the reinforcement peaks with (111) (202) (113) planes but it is observed for the samples contain 6 and 8 wt. % of ZrO<sub>2</sub> particles. It is observed that the composite sample contain low weight percentage of reinforcement not showed the any reinforcement peak. Aluminium peaks are observed in (111), (200), (220) and (311) planes for all the sample tested and these matched with JCPDS file #04-0787 data.

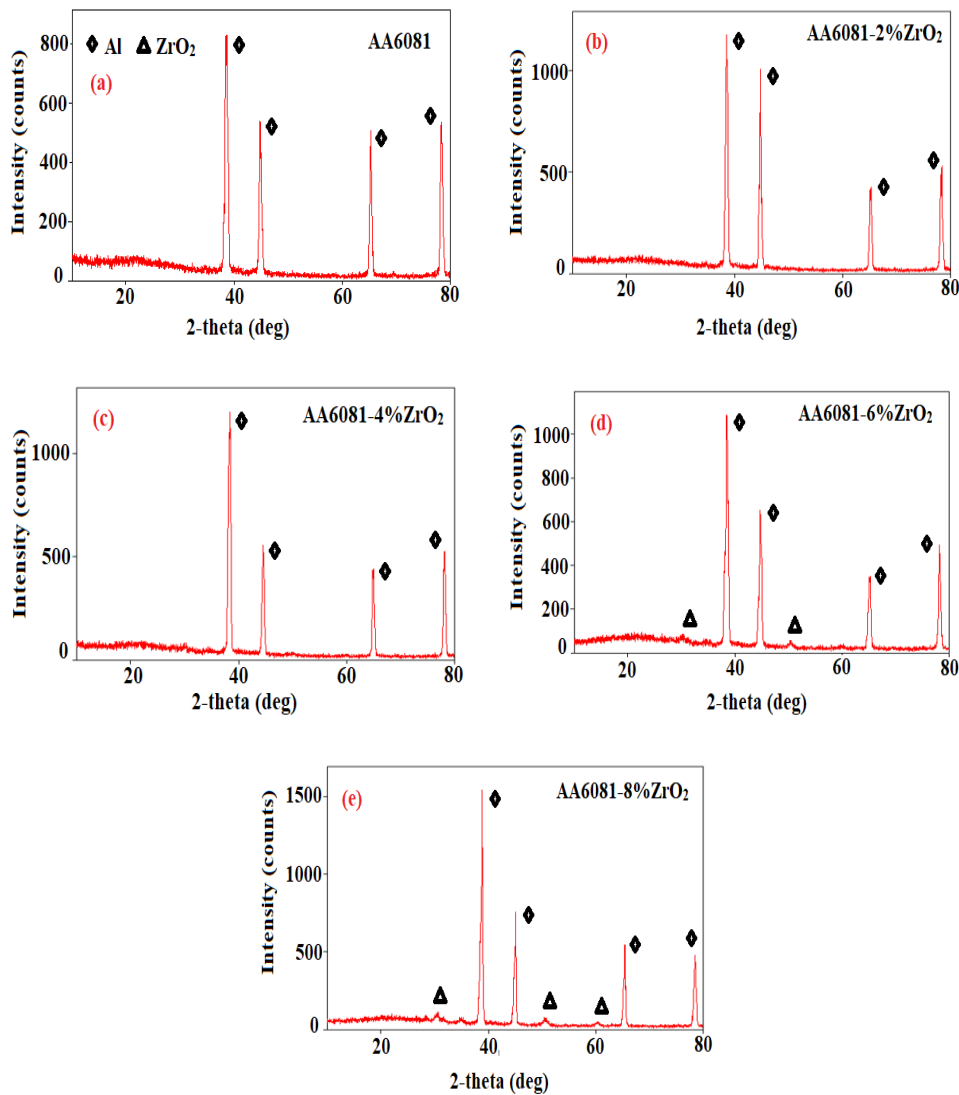


Fig. 5. (a-e) XRD analyses of sintered AA6081 and composite samples.

### 3.3. Effect of ZrO<sub>2</sub> on density of the composites

The outcome of ZrO<sub>2</sub> content on the theoretical and experimental density of composite samples after sintering is shown in Figure 6. The addition of ZrO<sub>2</sub> to the AA6081 matrix makes the composite samples denser. As the ZrO<sub>2</sub> content of the samples is increased, the theoretical and experimental density of the samples increases. The explanation for this is that the ZrO<sub>2</sub> particles have a higher density (5.68 g/cc) than the Aluminium matrix. For all of the samples analyzed, the observed experimental density is lower than the theoretical density. The effect of the amount of ZrO<sub>2</sub> content on the green density and porosity of the samples is shown in Figure 7. Because of the increased reinforcement material, the green density also increases. But the green density values are less than the sintered density. This is due to the higher mass of the green compacts. The effect of porosity shows the increasing trend. The addition of reinforcement increases the porosity for the composite samples [25].

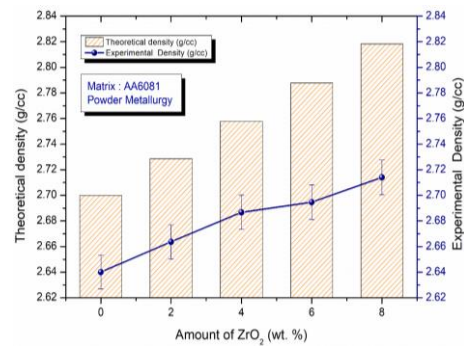


Fig. 6. Effect of amount of ZrO<sub>2</sub> content on theoretical and experimental density.

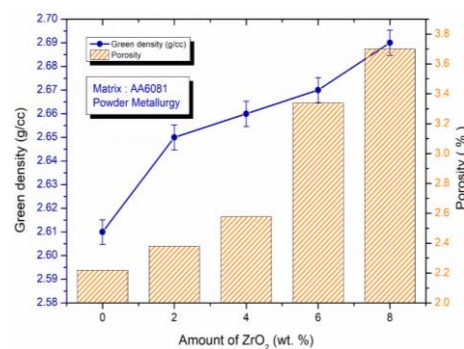


Fig. 7. Effect of amount of ZrO<sub>2</sub> content on green density and porosity.

### 3.4. Effect of ZrO<sub>2</sub> on hardness of the composites

The consequence of ZrO<sub>2</sub> content on composite sample hardness is depicted in Figure 8. For the composite samples, an increase in hardness was obtained. The composite samples' hardness was enhanced by incorporating hard ZrO<sub>2</sub> particles into the soft AA6081 matrix. The composite with 8 wt.% ZrO<sub>2</sub> particles had the highest hardness value. The AA6081 without reinforcement had the lowest hardness rating. The aim of this research is to use ZrO<sub>2</sub> particles to enhance the mechanical properties of the composite. The hardness of ZrO<sub>2</sub> particles improved the composite's hardness property [6]. PM process is the suitable route to fabricate the ZrO<sub>2</sub> distributed AA6081 composite with good mechanical property [16].

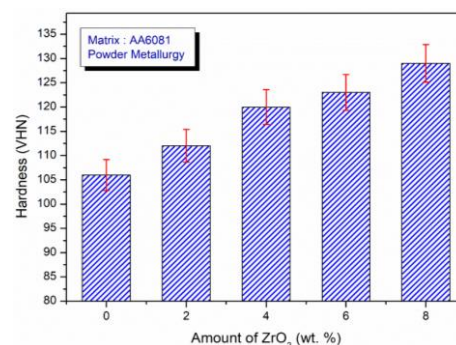


Fig. 8. Effect of amount of ZrO<sub>2</sub> content on hardness.

### 3.4. Effect of ZrO<sub>2</sub> on compressive strength of the composites

Figure 9 depicts the impact of ZrO<sub>2</sub> material on the CS of composite samples. As compared to unreinforced AA6081, the composite samples showed an increase in CS. The CS of

the composite samples was increased by incorporating hard  $ZrO_2$  particles into the soft AA6081 matrix. The CS of the composite containing 8%  $ZrO_2$  particles is higher than the CS of the other samples tested. The unreinforced AA6081 was found to have the lowest CS. The hardness of  $ZrO_2$  particles increased the composite's compressive strength [26].

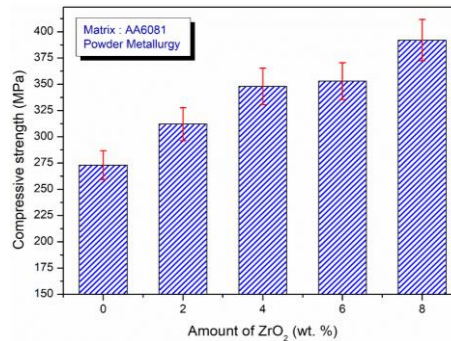


Fig. 9. Effect of amount of  $ZrO_2$  content on compressive strength.

### 3.5. Wear Behavior of the AA6081-8 wt. % $ZrO_2$ PM composite

In this section the wear behavior of the AA6081-8 wt. %  $ZrO_2$  PM composite. Here the AA6081-8 wt. %  $ZrO_2$  composite was selected for the wear studies as it has better mechanical properties among the tested composite samples. SN ratio values are provided in Table 3. The rank is provided based on the delta values. The P has the greatest influence on the WR, followed by D and V. Table 4 shows the mean values, and the parameters are ranked in the same order. Figure 10 shows the SN ratio graph for WR and Figure 11 shows the mean plot for WR. From the figure 11, the optimal parameters are identified for lower WR as  $A_1B_2C_1$  and which shows that low P, medium D and low V values would provide low WR for the AA6081-8 wt. %  $ZrO_2$  PM composite.

Table 3. SN Ratio table for wear rate.

Level	P(A)	D (B)	V (C)
1	-16.31	-16.59	-16.56
2	-16.73	-16.54	-16.64
3	-16.82	-16.72	-16.66
Delta	0.52	0.18	0.10
Rank	1	2	3

Table 4. Mean table for wear rate.

Level	P(A)	D (B)	V (C)
1	6.537	6.757	6.730
2	6.860	6.717	6.797
3	6.937	6.860	6.807
Delta( $\Delta$ )	0.400	0.143	0.077
Rank	1	2	3

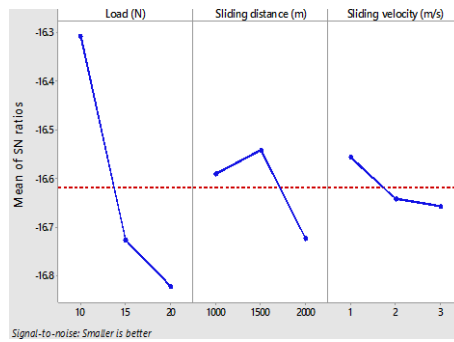


Fig. 10. SN ratio plot for wear rate.



Fig. 11. Mean plot for wear rate.

The contour plot between P and D for the WR of the AA6081- 8 wt. percent ZrO<sub>2</sub> PM Composite is shown in Figure 12. For the low P (10 N) and low D, the WR is low (1000 m). An increase in D raises the composite's WR, and an increase in P does the same. The reason is that the increase in P increases the penetration of the pin which is made by the hardened steel which ploughs the surface. Increase in D also lead to more WR of the composite because of rise in temperature on the surface between the pin and composite sample [27].

Figure 13 shows the contour plot between P and V for the WR of the AA6081- 8 wt. % ZrO<sub>2</sub> PM Composite. The low WR is observed for the low P (10 N) and medium V (2 m/s). Increase in V increases the WR of the composite and then decreases. The low WR was observed for the V of 2 m/s. Low level of P with medium V of the parameters provided the optimum WR. Since the temperature between the pin and the composite sample surface rises as V rises, more WR of the composite is generated [28]. The WR of the AA6081- 8 wt. percent ZrO<sub>2</sub> PM composite is shown in Figure 13 as a contour plot between D and V. The WR of the composite increases as D increases. Low WR is observed for the sample when the D is low and V is medium.

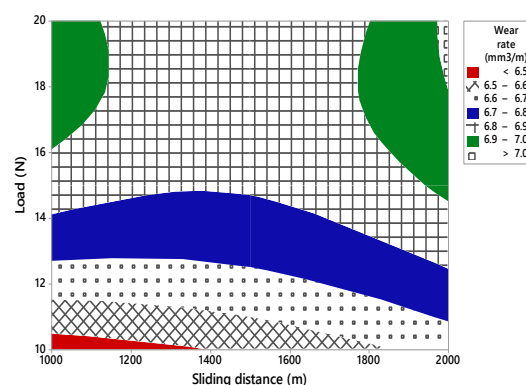


Fig. 12. Contour plot for wear rate (P & D).

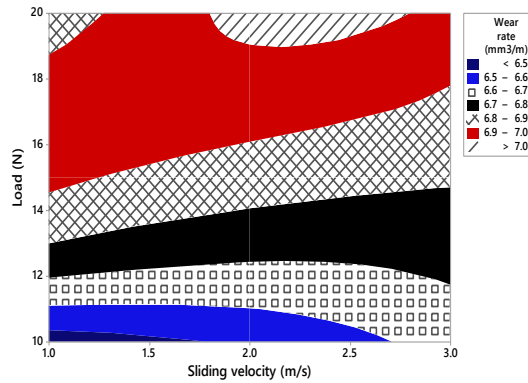


Fig. 13. Contour plot for wear rate (P & V).

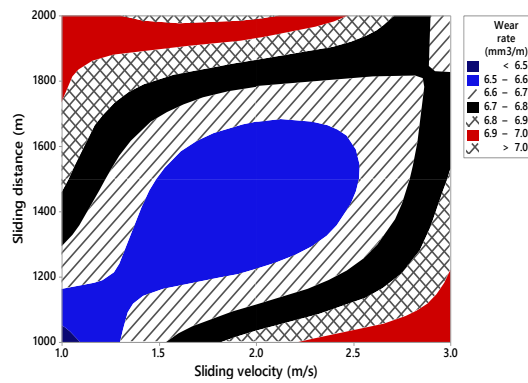


Fig. 14. Contour plot for wear rate (D & V).

Table 5 displays the ANOVA results for WR of the AA6081- 8 wt. % ZrO<sub>2</sub> PM composite. Table shows the adjacent sum square, adjacent mean square, F value and P value. From the table it is seen that P is the highly influenced factor and the contribution % is 85.37. Next to the P, D is the influencing parameter on the WR. This analysis is valid since the obtained error percentage is 0.98. The regression equation for the WR is provided in equation 1. Figure 15 shows the normal probability plot for the WR of the AA6081- 8 wt. % ZrO<sub>2</sub> PM composite sample. From the plot it is clear that the residuals are within the limit.

Table 5. ANOVA table for wear rate.

Parameter	DF	Adj.SS	Adj.MS	F-value	p-value	Contribution (%)
P (N)	2	0.270422	0.135211	87.55	0.011	85.37
D (m)	2	0.032822	0.032822	10.63	0.086	10.36
V (m/s)	2	0.010422	0.010422	3.37	0.229	3.29
Residual error	2	0.003089	0.003089			0.98
Total	8					100

$S = 0.0392994$ ;  $R-Sq = 99.02\%$ ;  $R-Sq(adj) = 96.10\%$ ;  $R-Sq(pred) = 80.25\%$   
 Wear rate (mm<sup>3</sup>/m) = 6.7778 - 0.2411 A<sub>1</sub> + 0.0822 A<sub>2</sub> + 0.1589 A<sub>3</sub> - 0.0211 B<sub>1</sub> - 0.0611 B<sub>2</sub> + 0.0822 B<sub>3</sub> - 0.0478 C<sub>1</sub> + 0.0189 C<sub>2</sub> + 0.0289 C<sub>3</sub> ----- (1)

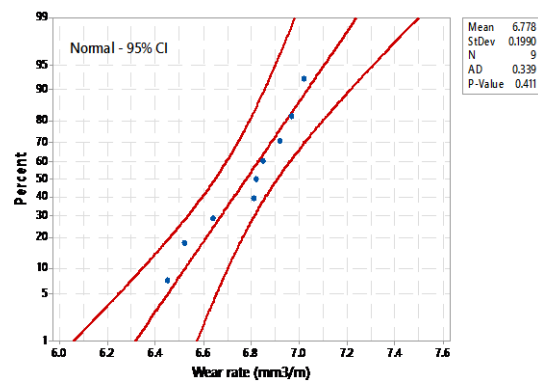


Fig. 15. Probability plot for wear rate.

#### 4. Conclusions

Powder metallurgy was used to successfully create an AA6081 matrix reinforced with ZrO<sub>2</sub> particles. The even disseminations of ZrO<sub>2</sub> particles in AA6081 alloy evident through SEM images. The accumulation of ZrO<sub>2</sub> particles improved the composites' hardness and compressive strength.

The wear behavior of the AA6081-8 wt. percent ZrO<sub>2</sub> PM composite was studied using the Taguchi technique. For the best wear rate, use the following parameters: load: 10 N, sliding distance: 1500 m, and sliding velocity: 1 m/s. The ANOVA results exposed that load had the greatest influence on composite wear rate, with a percentage contribution.

#### References

- [1] N. Mathan Kumar, S. Senthil Kumaran, L. A. Kumaraswamidhas, J. Alloys Compd. **652**, 244 (2015).
- [2] E. A. M. Shalaby, A. Y. Churyumov, A. N. Solonin, A. Lotfy, Mater. Sci. Eng. A. **674**, 18 (2016).
- [3] C. S. Ramesh, S. Pramod, R. Keshavamurthy, Mater. Sci. Eng. A **528**, 4125 (2011).
- [4] B. Ashok Kumar, N. Murugan, Mater. Des. **40**, 52 (2012).
- [5] S. Kumar, S. Ramanathan, S. Sundarrajan, Integr. Med. Res. **4**, 333 (2015).
- [6] K. Ravi Kumar, T. Pridhar, V. S. Sree Balaji, J. Alloys Compd. **765**, 171 (2018).
- [7] M. Roosta, H. Baharvandi, H. Abdizade, Int. J. Refract. Met. Hard Mater. **29**, 710 (2011).
- [8] S. A. Sajjadi, H. R. Ezatpour, M. Torabi Parizi, Mater. Des. **34**, 106 (2012).
- [9] M. Sumathi, N. Selvakumar, R. Narayanasamy, Mater. Des. **39**, 1 (2012).
- [10] H. Yang, R. Luo, Wear **270**, 675 (2011).
- [11] H. Wang, R. Zhang, X. Hu, C.A. Wang, Y. Huang, J. Mater. Process. Technol. **197**, 43 (2008).
- [12] M. Hrairi, M. Ahmed, Y. Nimir, Adv. Powder Technol. **20**, 548 (2009).
- [13] J. Corrochano, J. C. Walker, M. Lieblich, J. Ibáñez, W. M. Rainforth, Wear **270**, 658 (2011).
- [14] B. A. Cook, J. S. Peters, J. L. Harringa, A. M. Russell, Wear **271**, 640 (2011).
- [15] F. Akhlaghi, A. Zare-Bidaki, Wear **266**, 37 (2009).
- [16] N. Nemati, R. Khosroshahi, M. Emamy, A. Zolriasatein, Mater. Des. **32**, 3718 (2011).
- [17] M. Rahimian, N. Parvin, N. Ehsani, Mater. Sci. Eng. A **527**, 1031 (2010).
- [18] M. Ravichandran, V. Anandkrishnan, J. Mater. Res. **30**, 2380 (2015).
- [19] S. V. Alagarsamy, M. Ravichandran, Ind. Lubr. Tribol. **71**, 1064 (2019).
- [20] H. Beygi, M. Zare, S. A. Sajjadi, Powder Technol. **232**, 49 (2012).
- [21] M. Abdellahi, M. Bhmanpour, M. Bahmanpour, Ceram. Int. **40**, 16259 (2014).

- [22] K. Shiva Kumar, A. Chennakesava Reddy, *Results Mater.* **5**, 100070 (2020).
- [23] D. Srinivasan, M. Meignanamoorthy, M. Ravichandran, *Mater. Res. Express.* **6**, 076504 (2019).
- [24] B. Stalin, G. T. Sudha, M. Ravichandran, *Silicon* **10**, 2663 (2018).
- [25] G. B. V. Kumar, P. P. Panigrahy, S. Nithika, R. Pramod, C. S. P. Rao, *Compos. Part B Eng.* **175**, 107138 (2019).
- [26] V. Mohanavel, M. Ravichandran, *Mater. Res. Express.* **6**, (2019).
- [27] S. V. Alagarsamy, M. Ravichandran, *Mater. Res. Express.* **7**, (2020).
- [28] T. Rajmohan, K. Palanikumar, S. Ranganathan, *Trans. Nonferrous Met. Soc. China* **23**, 2509 (2013).
- [29] R.B.Durairaj , S.Ramachandran , G Mageshwaran , J Jeyajeevahan , G Brittojoseph , “ Investigations on Mechanical Properties of Titanium reinforced glass ionomer cement (GiC) – Ceramic Composite suitable for Dental Implant Applications in Digest journal of \ Nanomaterials and Bio-structures Volume 16, No 1, Issue 1, Jan-March 2021
- [30] Arunkumar T, Anish M, J Jayaprabakar, Jeya Jeevahan & Durairaj RB (2020) Study on Mechanical properties of polyurea coating with various process parameters, *Materials Research Innovations*, DOI: 10.1080/14328917.2020.1782078
- [31] Venkatesh Subramanian, DURAIRAJ R. B., MAGESHWARAN G, PRAKASH S, Deeraj B, Dheeban S. “Experimental Investigation on Mechanical Erosion and Permeation Behavior Of Plasma Nitriding over Manet Steel” Presented In FAME 2020 and Published In AIP Conference Proceedings MS ID: AIPCP20-AR-FAME2020-00134
- [32] Durairaj R B, Jeya Jeevahan Jayaraj, Jayaprakash Venugopal, Sriram Venkateswaran, and Britto Joseph G “”Mechanical behaviour and corrosion behaviour of SS316L and SS304 weldment in hanks solution” Presented In FAME 2020 And Published In AIP Conference Proceedings MS ID: AIPCP20-AR-FAME2020-00141
- [33] R B Durairaj , G Mageshwaran, J Jeyajeevahan , Madhu chereyala “Surface roughness and corrosion characterization of Multi walled carbon nano tube reinforced Zirconium composite coated over SS316L “ in ” in *International Journal of Ambient Energy* published by Taylor and Francis publications in September 2016 DOI:10.1080/01430750.2016.1237891.